ARTICLES

Nucleon spin fluctuations and neutral-current interactions in supernovae

Günter Sigl
Max-Planck-Institut für Physik, Föhringer Ring 6, D-80805 München, Germany
and Department of Astronomy and Astrophysics, The University of Chicago, Chicago, Illinois 60637-1433
(Received 10 March 1997)

The formation of neutrino spectra in a supernova depends crucially on the strength and inelasticity of weak interactions in hot nuclear matter. Neutrino interactions with nonrelativistic nucleons are mainly governed by the dynamical structure function for the nucleon spin-density which describes its fluctuations. These fluctuations give rise to inelastic weak processes such as neutrino pair emission and absorption as well as energy transfers in neutrino-nucleon scattering that can be comparable or greater than that from ordinary recoil. We calculate numerically the spin-density structure function in the limit of a dilute, nondegenerate medium from exact two-nucleon wave functions for some representative nuclear interaction potentials. We show that spectrum and magnitude of the energy transfer between neutrinos and nucleons can deviate significantly from those based on the Born approximation. They are, however, rather insensitive to the particular nuclear potential as long as it reproduces experimental nucleon scattering phase shifts at corresponding energies. We also compare with calculations based on a one-pion exchange potential in Born approximation and discuss their applicability in the context of supernovae. Our study is relevant for numerical simulations of the neutrino spectra emerging from type-II supernovae. [S0556-2821(97)03918-0]

PACS number(s): 97.60.Bw, 13.15.+g, 14.60.Lm, 95.30.Cq

I. INTRODUCTION

The detection of roughly a dozen neutrinos from SN 1987A is in good qualitative agreement with the neutrino signal expected from the early cooling phase of a hot neutron star born in the center of the collapsed core of a massive star [1]. It is therefore generally believed that type-II supernovae such as SN 1987A are the optical counterparts of such catastrophic events.

The formation of the spectra of neutrinos emitted from a type-II supernova takes place around the ''neutrinosphere'' where weak neutral-current scattering and pair processes involving electron, muon, and τ neutrinos, and charged current creation and absorption of electron neutrinos on nucleons, nuclei and electrons cease to be efficient in keeping the neutrinos in thermodynamical equilibrium with the medium. The interplay between (roughly) energy conserving scattering and processes changing neutrino numbers and energies plays a crucial role in that respect [2]. In previous studies of neutrino transport, the lowest order neutrino opacities in vacuum have been used. Neutral-current scattering processes on nucleons and nuclei have been approximated to be elastic [3]. As a result, whereas the energy fluxes predicted for the three neutrino flavors turn out to be very similar [2], the effective temperatures are significantly higher for muon and τ neutrinos compared to electron neutrinos which because of their more efficient energy exchange with the medium decouple from it further out.

However, weak interaction rates in a medium differ significantly from those taking place in vacuum. On the one hand, the spin-dependent strong force between nucleons establishes spatial correlations of the density and the spin-density in the medium that can either enhance or reduce average interaction rates. Many papers on weak interactions in neutron stars investigated these effects. However, they either applied the Landau theory of quasiparticles assuming a ''cold'' nuclear medium [4,5] or the authors focused on quasielastic scattering [4,6,7] for which the energy transfer to the nucleons is smaller than the momentum transfer.

On the other hand, a weak interaction transferring an energy ω to the medium is sensitive to the fluctuation power in density and spin-density at that frequency. For example, at finite density, the spin-dependent nucleon-nucleon interaction also causes the nucleon spins to fluctuate. This leads to a reduction of the average total axial-vector current neutrino scattering cross section compared to its vacuum value [8,9]. This effect is most important at the high temperatures pertaining in the first few seconds after formation of the hot neutron star. The nucleon spin fluctuations also lead to bremsstrahlung emission and absorption of neutrino pairs which can play an important role in the creation of thermal neutrinos inside the neutrinospheres. In addition, the fluctuating nucleon spins can, apart from recoil, imply an enhanced energy transfer in neutrino-nucleon scattering [10]. It is these inelastic neutral-current processes which we are mostly concerned with in the present work because they play a dominant role in the formation of neutrino spectra. Inelastic neutrino-nucleon scattering, for example, tends to decrease predicted effective temperatures of muon and τ neutrinos [2]. This is of some importance in view of new neutrino detectors such as Super-Kamiokande and the Sudbury Neutrino Observatory, which have the capability of measuring the neutrino spectra from nearby supernova events with much better statistics than is available with the data from SN 1987A.

Near the neutrinosphere the neutrino opacities are governed mainly by the local nucleon spin-density. Within linear response theory, weak neutral-current interactions are then determined by the dynamical structure function for the nucleon spin-density which describes its spatial and temporal correlations and is a function of energy and momentum transfer. For energy transfers that are larger than the typical spin fluctuation rate multiple nucleon-nucleon scattering is negligible, and, to lowest order in the nucleon-nucleon interaction, the spin-density structure function can be calculated from the matrix element for nucleon bremsstrahlung. This matrix element has been discussed in some detail in the literature [11–13] for a one-pion exchange (OPE) potential to lowest order in the pion-nucleon coupling, i.e., in Born approximation.

However, the Born approximation is only applicable if at least one of the following conditions is satisfied [14]:

$$|V| \ll \frac{1}{m_N a^2}, \quad |V| \ll \frac{p}{m_N a}, \tag{1}$$

where $|V| \sim 100$ MeV is the typical magnitude of the nuclear interaction potential, $a \sim 1$ fm is its range, p is the nucleon momentum in the center of mass system, and m_N is the free nucleon mass. The first condition is always violated if the potential leads to bound states as for the proton-neutron interaction which gives rise to the deuteron bound state. The second condition translates into $p \gtrsim m_N$ and is therefore also violated for the nonrelativistic nucleon momenta occurring in a supernova. We can therefore not expect that the Born approximation is a reliable approximation to the dynamical nucleon spin-density structure function in a supernova. Neither is it obvious that any weak interaction rates calculated from it are reliable at the relatively low energies involved.

The goal of this paper is therefore to compute the dynamical nucleon spin-density structure function and resulting weak interaction rates beyond the Born approximation by using exact two-nucleon wave functions. To keep things numerically simple, we will restrict ourselves to spherically symmetric but spin-dependent two-nucleon potentials. Since a central potential conserves the total nucleon spin, the only contribution to inelastic weak processes (i.e., inelastic in the center-of-mass frame of the nucleons) will then arise from interactions of protons and neutrons due to their different weak coupling constants. We therefore have to deal with two nucleon species. Our approach takes into account in a consistent, unified way the free-free transitions

$$\nu + n + p \leftrightarrow \nu + n + p \tag{2}$$

as well as the free-bound and bound-free processes involving the deuteron

$$\nu + d \leftrightarrow \nu + p + n. \tag{3}$$

The analogous processes involving neutrino pairs or axions instead of neutrino scattering are described by the same dynamical structure function and can therefore also be treated by our formalism.

The rest of the paper is organized as follows. In Sec. II we define the nucleon spin-density structure function in a form suitable for the case of proton-neutron interactions. The main formalism for computing this structure function from two-nucleon wave functions is presented in Sec. III. In Sec. IV the Born approximation is derived as a limiting case. Section V introduces a central potential which reproduces experimental data on proton-neutron scattering at energies below a few tens of MeV. The corresponding spin-density structure function and resulting weak interaction rates are calculated numerically for conditions near the neutrinosphere and compared with the Born approximation and calculations for an OPE potential. Finally, we summarize and conclude in Sec. VI. We use natural units, i.e., $c = \hbar = 1$, throughout this paper.

II. THE NUCLEON SPIN-DENSITY STRUCTURE FUNCTION

A. Definition and general properties

The main process of interest here, neutral-current neutrino-nucleon interaction, is given by the Hamiltonian

$$\mathcal{H}_{\rm int} = \frac{G_F}{2\sqrt{2}} \sum_{i=n,p} \overline{\psi_i} \gamma_\mu [C_{V,i} - C_{A,i}\gamma_5] \psi_i \overline{\psi_\nu} \gamma^\mu (1-\gamma_5) \psi_\nu, \tag{4}$$

where G_F is the Fermi constant, ψ_i $(i = n,p)$, and ψ_ν are the Dirac field operators for the neutrons, protons, and neutrinos, and $C_{V,i}$ and $C_{A,i}$ are the dimensionless weak neutral-current vector and axial-vector coupling constants for protons and neutrons, respectively.

Another possible type of weak process is the emission of axions [15]. The corresponding interaction Hamiltonian reads

$$\mathcal{H}_{\rm int} = \frac{1}{2 f_a} \sum_{i=n,p} C_{a,i} \overline{\psi_i} \gamma_\mu \gamma_5 \psi_i \partial^\mu a, \tag{5}$$

where a is the axion field, f_a the Peccei-Quinn scale, and the dimensionless coupling constants to neutrons and protons $C_{a,i}$ $(i = n,p)$ are of order unity and depend on the specific axion model.

In the limit of nonrelativistic nucleons, only the axial-vector coupling contributes to inelastic weak processes. Within linear response theory these processes are then described exclusively by the dynamical structure function for the nucleon spin-density. In the following, we will drop the index A or a in the nucleon coupling constants to neutrinos and axions, respectively, for notational simplicity whenever the result applies to both cases. To ensure a suitable normalization which will become clear below in Eq. (8), we define the structure function as the autocorrelation function of the weighted nucleon spin-density:

$$\boldsymbol{\sigma}_w(x) \equiv \sum_{i=n,p} \frac{C_i}{C} \phi_i^\dagger(x) \frac{\boldsymbol{\tau}}{2} \phi_i(x). \tag{6}$$

Here, $\phi_i(x)$ $(i = n,p)$ is the nonrelativistic field operator for protons and neutrons which is a Pauli two-spinor, $\boldsymbol{\tau}$ is the vector of Pauli matrices, and $C^2 \equiv C_n^2 Y_n + C_p^2 Y_p$ is an average neutral-current axial-vector weak coupling constant to the nucleons, weighted by the fractional neutron and proton abundances Y_n and Y_p. Defining the Fourier

transform in a normalization volume V as $\boldsymbol{\sigma}_w(t,\mathbf{k}) = V^{-1/2}\int d^3\mathbf{r} e^{-i\mathbf{k}\cdot\mathbf{r}}\boldsymbol{\sigma}_w(t,\mathbf{r})$, one can then define the nucleon spin-density structure function [13,10,16]:

$$S_\sigma(\omega,\mathbf{k}) = \frac{4}{3n_b}\int_{-\infty}^{+\infty} dt e^{i\omega t}\langle \boldsymbol{\sigma}_w(t,\mathbf{k})\cdot\boldsymbol{\sigma}_w(0,-\mathbf{k})\rangle. \quad (7)$$

Here, $(\omega,\mathbf{k})$ is the four-momentum transfer to the medium, n_b is the baryon number density, and the expectation value $\langle\cdots\rangle$ is taken over a thermal ensemble at the medium temperature T of medium states normalized to unity.

Relativistic neutrinos and possibly axions will have typical energies of order $3T$ but are in general not in chemical equilibrium with the medium. Weak interactions such as neutral-current neutrino scattering and pair processes and axion emission thus probe the spin-density function typically at thermal energy-momentum transfers. Since the momenta involved in the nucleon-nucleon interactions are much larger than the thermal momenta of relativistic particles, we will often employ the long wavelength limit $S_\sigma(\omega) \equiv \lim_{\mathbf{k}\to 0} S_\sigma(\omega,\mathbf{k})$ for which we define the dimensionless quantity $\widetilde{S}_\sigma(x) \equiv TS_\sigma(xT)$. In this limit, integration of Eq. (7) over ω yields the sum rule

$$\int_{-\infty}^{+\infty}\frac{d\omega}{2\pi}S_\sigma(\omega) - 1 = N_\sigma \equiv \frac{4}{3n_bV}\left\langle \sum_{i\neq j} \boldsymbol{\sigma}_{i,w}\cdot\boldsymbol{\sigma}_{j,w}\right\rangle, \quad (8)$$

where we wrote the spatial integral $\int d^3\mathbf{r}\boldsymbol{\sigma}_w(t,\mathbf{r}) = \Sigma_i \boldsymbol{\sigma}_{i,w}$. Here, $\boldsymbol{\sigma}_{i,w} \equiv \boldsymbol{\sigma}_i \mathrm{diag}(C_p,C_n)/C$, where $\boldsymbol{\sigma}_i$ are the spin operators of the individual nucleons, and the matrix $\mathrm{diag}(C_p,C_n)$ acts in isospin space. In Eq. (8) N_σ describes correlations among different nucleon spins. In the absence of such correlations $\int_{-\infty}^{+\infty}(d\omega/2\pi)S_\sigma(\omega)$ reduces to 1 which motivated the introduction of the weighted spin operator Eq. (6).

We formally introduce the complete set of eigenfunctions $|n\rangle$ of the total Hamiltonian H of the nuclear medium $H|n\rangle = \omega_n|n\rangle$, where ω_n are the corresponding energy eigenvalues. By inserting the identity operator $I = |n\rangle\langle n|$ between the spin operators, Eq. (7) can be rewritten into

$$S_\sigma(\omega,\mathbf{k}) = \frac{8\pi}{3n_b}\frac{1}{Z}\sum_{n,m} e^{-\omega_n/T}\,|\langle n|\boldsymbol{\sigma}_w(0,\mathbf{k})|m\rangle|^2 \times \delta(\omega+\omega_n-\omega_m), \quad (9)$$

where $Z = \Sigma_n e^{-\omega_n/T}$ is the partition function. This form will be useful later and it shows that the structure function satisfies detailed balance:

$$S_\sigma(\omega,\mathbf{k}) = S_\sigma(-\omega,-\mathbf{k})e^{\omega/T}. \quad (10)$$

It is therefore sufficient to know the function, e.g., for positive energy transfer to the medium, $\omega \geqslant 0$.

Up to now no approximations have been made with regard to the nucleon-nucleon interactions which determine the nonperturbative though unknown structure function $S_\sigma(\omega,\mathbf{k})$. From now on we will make the assumption that only two-nucleon forces are present. The Hamiltonian then has the form

$$H = \sum_i \frac{\mathbf{p}_i^2}{2m_N} + \frac{1}{2}\sum_{i\neq j} V(\mathbf{r}_{ij},\boldsymbol{\sigma}_i,\boldsymbol{\sigma}_j), \quad (11)$$

where $\mathbf{r}_{ij}$ is the radius vector between nucleon i and j, $\mathbf{p}_i$ is the nucleon momentum, $V(\mathbf{r}_{ij},\boldsymbol{\sigma}_i,\boldsymbol{\sigma}_j)$ is the spin-dependent two-nucleon interaction potential, and the sums run over all nucleons. The most general two-nucleon potential in the nonrelativistic limit can be written as [17]

$$V(\mathbf{r},\boldsymbol{\sigma}_1,\boldsymbol{\sigma}_2) = U(r) + U_\sigma(r)\boldsymbol{\sigma}_1\cdot\boldsymbol{\sigma}_2 + U_T(r)T_{12} + P_\tau[U^\tau(r) + U^\tau_\sigma(r)\boldsymbol{\sigma}_1\cdot\boldsymbol{\sigma}_2 + U^\tau_T(r)T_{12}], \quad (12)$$

where $\mathbf{r} = \mathbf{r}_{12}$, $r = |\mathbf{r}|$, $\hat{\mathbf{r}} = \mathbf{r}/r$, P_τ is the isospin exchange operator, and the tensor operator is given by

$$T_{12} = 3\boldsymbol{\sigma}_1\cdot\hat{\mathbf{r}}\boldsymbol{\sigma}_2\cdot\hat{\mathbf{r}} - \boldsymbol{\sigma}_1\cdot\boldsymbol{\sigma}_2. \quad (13)$$

Useful information about structure functions is contained in their moments of which Eq. (8) is an example for the lowest one. The next higher moment is given by the so-called f-sum rule which is often discussed in the literature in the context of the density structure function and for spin-conserving interactions [18]. In Ref. [16] we derived a generalized f-sum rule for the spin-density structure function for one species of nucleons interacting via spin-dependent forces of the form Eq. (12) in a nondegenerate medium:

$$\int_{-\infty}^{+\infty}\frac{d\omega}{2\pi}\,\omega S_\sigma(\omega) = -\frac{4}{n_bV}\langle H_T\rangle. \quad (14)$$

Here, H_T is the part of the total Hamiltonian involving the tensor operator T_{ij}. In the present paper we will consider both neutrons and protons but assume a central two-nucleon potential, i.e., absence of tensor contributions. The f-sum rule is then modified to

$$\int_{-\infty}^{+\infty}\frac{d\omega}{2\pi}\omega S_\sigma(\omega) = -\frac{4}{3n_bV}\left(\frac{C_p-C_n}{C}\right)^2\langle H^{np}_\sigma\rangle, \quad (15)$$

where H^{np}_σ is the spin-dependent central part of the total Hamiltonian which contributes to neutron-proton interactions. Note from Eqs. (10) and (14) that for only one nucleon species a tensor interaction is required to give a nontrivial spin-density structure function. This is because the central part of the interaction conserves the total nucleon spin and thus does not contribute to its fluctuations. In contrast, for two nucleon species, a central spin-dependent proton-neutron interaction is sufficient for a nontrivial structure function as long as the neutral-current axial-vector weak coupling constants for protons and neutrons are different [see Eq. (15)]. We stress, however, that the actual (positive) value of the f sum depends on all interaction terms via the states entering the thermal average.

B. Relevance for weak interactions

The differential axial-vector-current neutrino-nucleon cross section is determined by the dynamical nucleon spin-

density structure function $S_\sigma(\omega,\mathbf{k})$, taken at the difference of initial and final neutrino four-momentum $(\varepsilon_1,\mathbf{k}_1)$ and $(\varepsilon_2,\mathbf{k}_2)$ via [13,16]

$$d\sigma_A = G_F^2 C_A^2 \frac{3-\cos\theta}{4} S_\sigma(\varepsilon_1-\varepsilon_2,\mathbf{k}_1-\mathbf{k}_2)\frac{d^3\mathbf{k}_2}{(2\pi)^3}, \quad (16)$$

where θ is the angle between $\mathbf{k}_1$ and $\mathbf{k}_2$. In our convention, the neutral-current axial-vector contribution to neutrino scattering rates on the ensemble of all nucleons is $n_b d\sigma_A$.

The volume emissivity of energy in axions, Q_a, is governed by a structure function $S_{\sigma,a}$ which is obtained from Eqs. (6), (7) by substituting $C_i \to C_{a,i}$ $(i=n,p)$:

$$Q_a = \frac{C_a^2 n_b}{(4\pi)^2 f_a^2}\int_0^\infty d\omega\,\omega^4 S_{\sigma,a}(-\omega,\omega), \quad (17)$$

where $C_a^2 \equiv C_{a,n}^2 Y_n + C_{a,p}^2 Y_p$. We have assumed an isotropic medium such that $S_\sigma(\omega,\mathbf{k})$ only depends on $k=|\mathbf{k}|$.

Various quantities relevant for neutrino interactions are determined by the spin-density structure function. For the remainder of this section, we assume a Maxwell-Boltzmann distribution at temperature T_ν for the neutrinos. Furthermore, we make use of the normalization given by Eq. (8). Contributions from spin-spin correlations represented by N_σ are mainly induced by the presence of nucleon bound states and by the Pauli exclusion principle which becomes important in a degenerate medium [19]. Both effects are small in the hot post-collapse phase of a supernova in which we are interested. Two-nucleon correlations, for example, can be evaluated within our numerical model, see Eq. (38) and Fig. 3 below, and typically result in $N_\sigma \lesssim 0.1$. To lowest order, we can therefore neglect N_σ in Eq. (8) when calculating the average energy transfer per collision in a dilute medium. It can then be written as [10,9]

$$\frac{\langle\Delta\varepsilon\rangle}{T} = \int_0^\infty \frac{dx}{2\pi}\,\widetilde{S}_\sigma(x)\left(x+\frac{\beta x^2}{2}+\frac{\beta^2 x^3}{12}\right)(e^{-\beta x}-e^{-x}), \quad (18)$$

with $\beta \equiv T/T_\nu$. This should be compared to the average energy transfer by nucleon recoils [20]:

$$\langle\Delta\varepsilon\rangle_{\rm recoil} = \frac{30(1-\beta)}{\beta^2}\frac{T^2}{m_N}. \quad (19)$$

Another interesting quantity is the reduction of the average total axial-vector current scattering cross section $\langle\sigma_A\rangle$ [see Eq. (16)] in the nuclear medium [8,9]. First we note that a term of the form $A\delta(\omega)$ in $S_\sigma(\omega)$ corresponds to a total elastic scattering cross section

$$\sigma_{\rm el}(\varepsilon_1) = \frac{3A}{8\pi^2} G_F^2 C_A^2 \varepsilon_1^2. \quad (20)$$

For $n_b \to 0$ there are no spin fluctuations and correlations, and Eq. (8) implies $S_\sigma(\omega) = 2\pi\delta(\omega)$ and thus $\sigma_0 \equiv (9/\pi) C_A^2 G_F^2 T^2$ for the thermally averaged cross section. In Ref. [9] we obtained the expression

$$\frac{\delta\langle\sigma_A\rangle}{\sigma_0} \equiv \frac{\langle\sigma_A\rangle-\sigma_0}{\sigma_0} = N_\sigma - \int_0^\infty \frac{dx}{2\pi}\,\widetilde{S}_\sigma(x) \times\left[1-\left(1+x+\frac{x^2}{6}\right)e^{-x}\right], \quad (21)$$

which again holds in the dilute medium.

Finally, we are interested in the rates of emission and absorption of neutrino pairs. The rate of emission per density of final neutrino states is given by $G_F^2 C_A^2 n_b (3+\cos\theta) S_\sigma(-\varepsilon_1-\varepsilon_2,-\mathbf{k}_1-\mathbf{k}_2)/4$ which leads to the volume emissivity of energy in neutrino pairs

$$Q_{\nu\bar\nu} = \frac{G_F^2 C_A^2 n_b}{160\pi^4}\int_0^\infty d\omega\,\omega^6 S_\sigma(-\omega), \quad (22)$$

where we have adopted the long wavelength approximation. The physical quantities discussed here will be calculated for the supernova environment in Sec. V.

III. BEYOND THE BORN APPROXIMATION

A. Classical versus general quantum result

In the limit $|\omega| \ll T$ the nucleon spin can be treated as a classical spin $\mathbf{s}$ being changed abruptly by some random amount $\Delta\mathbf{s}$ in a typical nucleon-nucleon collision event which takes place on a time scale $\simeq 1/T$ and thus appears to be ''hard.'' In this case we expect [21]

$$S_\sigma(\omega) \simeq \frac{\Gamma_\sigma}{\omega^2+\Gamma_\sigma^2/4}, \quad (23)$$

where the spin fluctuation rate Γ_σ is related to the collision rate $\Gamma_{\rm coll}$ by

$$\Gamma_\sigma = \frac{\langle(\Delta\mathbf{s})^2\rangle}{\langle\mathbf{s}^2\rangle}\,\Gamma_{\rm coll}. \quad (24)$$

Note that the spin fluctuation rate suppresses the ω^{-2} bremsstrahlung spectrum which otherwise would violate the existence of the normalization Eq. (8). This is known as the Landau-Pomeranchuk-Migdal (LPM) effect [22,23]. In previous work [24,25,10,16] it has been discussed how the Lorentzian shape Eq. (23) might influence weak interaction rates at high densities where $\Gamma_\sigma \gtrsim T$. The high-density behavior of the spin-density structure function can also influence limits on the axion mass [26].

For $|\omega| \gg \Gamma_\sigma$ multiple scattering effects can be ignored and the spin-density structure function can be computed by a quantum-mechanical treatment of two-nucleon scattering. From the generic ω^{-2} divergence of all bremsstrahlung processes for $\omega \to 0$ one expects the general form [9]

$$S_\sigma(\omega) = \frac{\Gamma_\sigma}{\omega^2} s(\omega/T)\begin{cases} e^{\omega/T} & \text{for} \quad \omega<0, \\ 1 & \text{for} \quad \omega>0, \end{cases} \quad (25)$$

where $s(x)$ is a nonsingular even function with $s(0)=1$. The specific shape of $s(x)$ for $x \gtrsim 1$ depends on the nucleon-nucleon interaction potential Eq. (12), and its calculation for realistic interaction potentials is the main goal of this paper.

Comparing Eqs. (23) and (25) in their common range of validity, $\Gamma_\sigma \ll |\omega| \ll T$, shows that the coefficient Γ_σ of the bremsstrahlung divergence in Eq. (25) can be interpreted as a nucleon spin fluctuation rate and that the classical limit of hard collisions corresponds to $s(x)=1$. The existence of the f-sum Eqs. (14), (15) shows that $s(x)$ has to decrease for large x due to quantum corrections.

B. Exact treatment in the limit of large energy transfers

For $\omega \gtrsim \Gamma_\sigma$ where scattering involving more than two nucleons is negligible, we can numerically compute two-nucleon wave functions from a given nucleon-nucleon interaction potential and use them in the general expression Eq. (9). For a central potential the eigenfunctions for the relative motion in the proton-neutron center-of-mass system

$$|P\rangle \equiv |p,l,m,S\rangle = R_{plS}(r) Y_{lm}(\Omega)|S\rangle \tag{26}$$

are characterized by the quantum numbers for the radial momentum p, the orbital angular momentum l and m, and the total spin S, where $R_{plS}(r)$ is the radial wave function and $Y_{lm}(\Omega)$ are the spherical harmonics. The corresponding energy eigenvalues ω_P have a $(2l+1)(2S+1)$-fold degeneracy. The Pauli exclusion principle then also determines the isospin to $I=\frac{1}{2}+(-1)^l(\frac{1}{2}-S)$. Assuming an isotropic medium and using $\boldsymbol{\sigma}_w(0,\mathbf{k}) = V^{-1/2}\Sigma_i \boldsymbol{\sigma}_i e^{-i\mathbf{k}\cdot\mathbf{r}_i} \mathrm{diag}(C_p, C_n)/C$ with a normalization volume $V=1/n_b$, after some algebraic manipulations we obtain

$$\begin{aligned} S_\sigma(\omega,k) = {} & \frac{16\pi^{1/2}}{3C^2} \frac{1}{k}\left(\frac{m_N}{T}\right)^{1/2} Y_p Y_n \frac{1}{Z_{CM}} \\ & \times \sum_{P,Q} e^{-\omega_P/T - m_N[\omega+\omega_P-\omega_Q-k^2/(4m_N)]^2/(Tk^2)} \\ & \times |\langle P| C_p \boldsymbol{\sigma}_p e^{-i(\mathbf{k}\cdot\mathbf{r}/2)} + C_n \boldsymbol{\sigma}_n e^{+i(\mathbf{k}\cdot\mathbf{r}/2)} |Q\rangle|^2, \end{aligned} \tag{27}$$

where $Z_{CM} = \Sigma_P e^{-\omega_P/T}$. For $k \to 0$ this expression transforms into

$$\begin{aligned} S_\sigma(\omega) = {} & 4\pi Y_p Y_n \left(\frac{C_p - C_n}{C}\right)^2 \frac{1}{Z_{CM}} \\ & \times \sum_{p,q} \sum_l (2l+1) \sum_{S=0}^{1} e^{-\omega_P/T} \\ & \times \left| \int_0^{r_{\max}} dr r^2 R^*_{plS}(r) R_{ql(1-S)}(r) \right|^2 \delta(\omega+\omega_P-\omega_Q), \end{aligned} \tag{28}$$

where we have made use of the orthogonality of the system of eigenfunctions which are supposed to be normalized to unity. In practice one constructs bound and scattering states of the stationary radial Schrödinger equation within a finite spherical volume of radius $r_{\max}$ and computes the matrix elements appearing in Eq. (28). For a nucleon interaction potential that is not radially symmetric, the eigenstates $|P\rangle \equiv |pJ\mathcal{P}\rangle$ are characterized by the total angular momentum J and parity $\mathcal{P}$ and are superpositions of orbital angular momentum eigenstates. With this modification, Eq. (27) still holds but we will not pursue this more complicated case here which would lead to coupled radial equations for the corresponding radial functions $R_{pJ\mathcal{P}}$.

Since we neglect interactions among more than two nucleons, our formalism does only account for neutrons, protons, and deuterons. Higher nuclei such as helium are not included. In this sense, strictly, n_b, Y_p, and Y_n have to be interpreted within the ensemble of neutrons, protons, and deuterons only. Nuclear statistical equilibrium (NSE) shows that in practice this does not make a big difference around and inside the neutrinosphere, as long as $Y_p \lesssim 0.3$ holds in addition, which is realistic after the first few hundred milliseconds after supernova core bounce. Keeping this in mind we can now calculate Z_{CM} analytically. Around the neutrinosphere the nucleons are at best mildly degenerate. We therefore assume a Maxwell-Boltzmann distribution $f(p) = e^{-p^2/(2\mu T)}$ for the unbound proton-neutron states. Here, $p = s^{1/2}/2$ is the nucleon momentum in the center-of-mass system, expressed in terms of the squared center-of-mass energy s (excluding the nucleon rest mass), and $\mu = m_N/2$ is the reduced nucleon mass. Taking into account the spin degrees of freedom we then have

$$Z_{CM} = 3e^{\varepsilon_d/T} + \frac{4}{n_b}\left(\frac{\mu T}{2\pi}\right)^{3/2}, \tag{29}$$

where $\varepsilon_d \simeq 2.2$ MeV is the deuteron binding energy (the deuteron has $S=1$). The degree of dissociation, i.e., the fractional abundance of unbound states is then

$$f_u = \left[1 + \frac{3}{4} n_b \left(\frac{2\pi}{\mu T}\right)^{3/2} e^{\varepsilon_d/T}\right]^{-1}. \tag{30}$$

As a consequence, $S_\sigma(\omega)$ from Eqs. (27) and (28) does not exhibit a simple linear scaling with the nucleon density n_b, except for the dilute limit $n_b \to 0$, $f_u \to 1$. It can be seen that the numerator in Eqs. (27) and (28) is independent of n_b and the density dependence of S_σ thus exclusively stems from Z_{CM}.

In the limit of zero temperature, $f_u \to 0$ and only the deuteron bound state will be populated in thermal equilibrium. In this limit, Eq. (16) describes the cross section for the weak neutral-current deuteron break-up process, Eq. (3). Integration over the phase space for the outgoing neutrino yields the total cross section

$$\sigma^{\mathrm{NC}}_{\nu d}(\varepsilon_1) = \frac{3G_F^2}{16\pi^2} \frac{(C_p - C_n)^2}{Y} \int_{\varepsilon_d}^{\varepsilon_1} d\omega (\varepsilon_1 - \omega)^2 [\lim_{T\to 0} S_\sigma(\omega)] \tag{31}$$

for incident neutrino energy ε_1.

Another instructive limiting case is the absence of spin-flip interactions. Scattering on protons and neutrons then has to be added incoherently with the states $|P\rangle$ now being plane waves. Equation (27) then reduces to the ordinary recoil expression

$$S_\sigma(\omega,k) = \frac{1}{k}\left(\frac{2\pi m_N}{T}\right)^{1/2} e^{-m_N[\omega - k^2/(2m_N)]^2/(2Tk^2)}. \tag{32}$$

Let us now get back to the general case. In agreement with Eq. (15) and Ref. [11] only proton-neutron scattering contributes to Eq. (28), and only if the neutral-current axial-vector weak coupling constants for protons and neutrons are different. Since the total spin is conserved by a central potential, the spin-density structure function is governed by the fluctuations of the difference of the proton and neutron spin $\boldsymbol{\sigma}_p-\boldsymbol{\sigma}_n$. To compare with the general results Eqs. (23) and (25), we study the corresponding spin-flip cross section which is defined as

$$\sigma_{\rm sf}(s)=\frac{\langle[\Delta(\boldsymbol{\sigma}_p-\boldsymbol{\sigma}_n)]^2\rangle}{\langle(\boldsymbol{\sigma}_p-\boldsymbol{\sigma}_n)^2\rangle}\sigma_{np}(s). \tag{33}$$

Here, $\sigma_{np}(s)\equiv\Sigma_l\sigma_{np}(l,s)$, where the average total proton-neutron scattering cross section in angular momentum state l is given by

$$\sigma_{np}(l,s)=\frac{4\pi}{s}(2l+1)[3\sin^2\delta_{l,1}(s)+\sin^2\delta_{l,0}(s)] \tag{34}$$

in terms of the phase shifts $\delta_{lS}(s)$. The latter are defined by the asymptotic behavior

$$R_{plS}(r)\propto\sin[(2\mu\omega_P)^{1/2}r-l\pi/2+\delta_{lS}(8\mu\omega_P)], \tag{35}$$

of the scattering states $\omega_P>0$ for $(2\mu\omega_P)^{1/2}r\gg l$. The nucleon spin-flip rate is now just defined as

$$\Gamma_{\rm sf}=Y_pY_nn_b\frac{\int_0^{+\infty}dpp^2f(p)(p/\mu)\sigma_{\rm sf}(4p^2)}{\int_0^{+\infty}dpp^2f(p)}, \tag{36}$$

where p/μ is the relative velocity of proton and neutron.

As can be seen from phase shift analysis, the spin-flip cross section Eq. (33) is

$$\sigma_{\rm sf}(s)=\frac{16\pi}{3s}\sum_l(2l+1)[\sin\delta_{l,1}(s)-\sin\delta_{l,0}(s)]^2. \tag{37}$$

Note that this vanishes if the phase shifts for $S=0$ and $S=1$ are equal, as expected. Given $\sigma_{\rm sf}$, one can compute $\Gamma_{\rm sf}$ from Eq. (36) and compare it with the Born approximation to be discussed below and with Eq. (25). This will be done in the following two sections.

Finally, one can calculate the spin-correlation term Eq. (8) that appears in the average cross-section reduction Eq. (21):

$$N_\sigma=Y_pY_n\frac{C_{A,p}C_{A,n}}{C_A^2}\frac{1}{Z_{CM}}\sum_p\sum_l(2l+1)\times\sum_{S=0}^{1}(-1)^{S(S+1)-1}e^{-\omega_P/T}, \tag{38}$$

which, together with Eq. (28), determines Eq. (21) in the phase shift treatment.

IV. THE BORN APPROXIMATION

By expanding the unbound states $|P\rangle$ into plane waves within first order perturbation theory and inserting the result into Eq. (27), one obtains the spin-density structure function in Born approximation. For $\omega>0$, the result in the long wavelength limit is

$$S_\sigma^{\rm Born}(\omega)=\frac{1}{\omega^2}\frac{\mu}{2\pi}Y_pY_nn_b\left(\frac{C_p-C_n}{C}\right)^2\times\frac{\int_0^{+\infty}dppf(p)\int_{k_{\rm min}}^{k_{\rm max}}dkk|U_\sigma^{np}(k)|^2}{\int_0^{+\infty}dpp^2f(p)}, \tag{39}$$

where $k_{\rm max,min}=(p^2+2\mu\omega)^{1/2}\pm p$, and $U_\sigma^{np}(k)$ is the Fourier transform of the coefficient of $\boldsymbol{\sigma}_p\cdot\boldsymbol{\sigma}_n$ in the proton-neutron interaction ($\boldsymbol{\sigma}_p$ and $\boldsymbol{\sigma}_n$ being the proton and neutron spins). Only the relative motion between proton and neutron influences Eq. (39) because neither energy nor momentum can be transferred to the center-of-mass motion in the long wavelength limit. In contrast to Eq. (28), $S_\sigma^{\rm Born}(\omega)$ scales linearly with n_b.

In Ref. [9] we considered one species of nucleons coupling to a classical, external scattering center via an interaction of the form Eq. (12) where one of the spins was replaced by a classical spin **s** associated with the external scatterer. The result for the spin-density structure function in the long wavelength limit in Born approximation is very similar to Eq. (39) for the case of a central two-nucleon potential and a medium of protons and neutrons with different neutral-current axial-vector weak coupling constants.

In Born approximation, the spin-flip cross section Eq. (33) evaluates to

$$\sigma_{\rm sf}^{\rm Born}(s)=\frac{20}{27\pi}\frac{\mu^2}{s}\int_0^{s^{1/2}}dkk|U_\sigma^{np}(k)|^2, \tag{40}$$

where $\langle(\boldsymbol{\sigma}_p-\boldsymbol{\sigma}_n)^2\rangle=3/2$ was used. Comparing Eqs. (25), (39), and (36) yields

$$\Gamma_\sigma^{\rm Born}=\frac{27}{10}\left(\frac{C_p-C_n}{C}\right)^2\Gamma_{\rm sf}^{\rm Born}, \tag{41}$$

i.e., the spin fluctuation rate in $S_\sigma(\omega)$ and the average spin-flip rate indeed agree within a factor of order unity, apart from the factor $[(C_p-C_n)/C]^2$ involving the weak coupling constants which results from our specific definition of S_σ.

As an example, we consider the usually adopted OPE potential which is a good approximation to the nucleon-nucleon interaction for distances greater than the inverse pion mass m_π. With $f\simeq1$ being the pion-nucleon coupling constant, its Fourier transform is

$$V_{\rm OPE}(\mathbf{k},\boldsymbol{\sigma}_1,\boldsymbol{\sigma}_2)=-\left(\frac{2f}{m_\pi}\right)^2\frac{(\boldsymbol{\sigma}_1\cdot\mathbf{k})(\boldsymbol{\sigma}_2\cdot\mathbf{k})}{k^2+m_\pi^2}(2P_\tau-1) \tag{42}$$

and it clearly has a tensor contribution. The spin-density structure function corresponding to this potential has been

calculated in Born approximation [13]. Translated into our notation, the contribution from proton-neutron scattering takes the form of Eq. (25) with $s(x)\equiv\tilde{s}(x)/\tilde{s}(0)$ given by the function

$$\tilde{s}(x)=\int_0^\infty dv[v(v+x)]^{1/2}e^{-v}\times[(5C_+^2+3C_-^2)s_1(v,x)+2(C_+^2+C_-^2)s_2(v,x)-(6C_+^2+2C_-^2)s_3(v,x)], \quad (43)$$

where $C_\pm=(C_p\pm C_n)/2$ and

$$s_i(v,x)=\int_{-1}^{+1}dz\begin{cases}\left(\dfrac{2v+x-2z[v(v+x)]^{1/2}}{2v+x-2z[v(v+x)]^{1/2}+y}\right)^2 & i=1,\\ \dfrac{(2v+x)^2-4v(v+x)z^2}{(2v+x+y)^2-4v(v+x)z^2} & i=2,\\ \dfrac{x^2}{(2v+x+y)^2-4v(v+x)z^2} & i=3,\end{cases} \quad (44)$$

with $y\equiv m_\pi^2/(m_N T)$. Furthermore, the contribution to the nucleon spin fluctuation rate Γ_σ is

$$\Gamma_{\sigma,\mathrm{OPE}}^{\mathrm{Born}}=\frac{2}{3}Y_pY_n\frac{\tilde{s}(0)}{C^2}\Gamma_A, \quad (45)$$

with

$$\Gamma_A=4\sqrt{\pi}\alpha_\pi^2\frac{n_bT^{1/2}}{m_N^{5/2}}=8.6\ \ \mathrm{MeV}\ \ \rho_{13}T_{10}^{1/2}. \quad (46)$$

Here, $\alpha_\pi\equiv(f2m_N/m_\pi)^2/4\pi\approx 15$, $\rho_{13}\equiv\rho/10^{13}$ g cm^{-3} with ρ the density, and $T_{10}\equiv T/10$ MeV. Note that $S_{\sigma,\mathrm{OPE}}^{\mathrm{Born}}(\omega)\propto\omega^{-3/2}$ for $\omega\to\infty$ and thus violates f-sum integrability. As was explained in Ref. [16], this is caused by the unphysical behavior of the OPE potential for $r\to 0$ that leads to a $|V_{\mathrm{OPE}}(\mathbf{k})|$ which for $k\to\infty$ is asymptotically constant [see Eq. (42)].

More generally, as can be seen from Eq. (39), one has $S_\sigma^{\mathrm{Born}}(\omega)\propto\omega^{-3/2-r}$ for $\omega\to\infty$ if $|U_\sigma(k)|\propto k^{-r}$ for $k\to\infty$, corresponding to existence and square integrability of the $(r-2)$th derivative of the interaction potential. It is not obvious whether this applies to the high ω behavior of the expression Eq. (28) as well.

V. A NUMERICAL MODEL FOR THE SUPERNOVA ENVIRONMENT

We first note that $S_\sigma(\omega)$ from Eqs. (39) and (27) is proportional to the dimensionless factor

$$Y\equiv Y_pY_n\left(\frac{C_p-C_n}{C}\right)^2=(C_p-C_n)^2\frac{Y_pY_n}{C_p^2Y_p+C_n^2Y_n}, \quad (47)$$

which describes its compositional and coupling constant dependence for fixed n_b and T. For processes involving only protons or neutrons this factor would be replaced by Y_p^2 and Y_n^2, respectively. Since interaction rates are proportional to n_bS_σ by definition, Y is a rough measure of the contribution of proton-neutron scattering to weak neutral-current inelastic interaction rates. For the neutrino-nucleon coupling in a nuclear medium we will adopt $C_{A,p}\simeq 1.09$ and $C_{A,n}\simeq -0.91$ [13], so that $Y\simeq 0.5$ for $Y_p\simeq 0.1$.

In the following we are interested in the situation given in the environment of the neutrinosphere in a supernova. In principle, our expressions for weak interaction rates depend on both density ρ and temperature T, apart from being proportional to Y. In order to reduce the number of independent parameters to 1 for simplicity, we will assume a specific profile for the temperature as a function of the density:

$$T(\rho)=5\left(\frac{\rho}{10^{13}\ \mathrm{g\,cm^{-3}}}\right)^{1/3}\mathrm{MeV}. \quad (48)$$

This profile is typical for the conditions in the supernova a few hundred milliseconds after core bounce. Under these circumstances, f_u varies between $\simeq 0.72$ at $\rho=10^{11}$ g cm^{-3} and $\simeq 0.16$ at $\rho=10^{14}$ g cm^{-3}, corresponding to a fractional deuterium abundance $Y_d\simeq(1-f_u)Y_p/[1-(1-f_u)Y_p]$. NSE involving higher nuclei gives deuterium abundances that are $20-30$ % lower than this if $Y_p\lesssim 0.2$, and $10-20$ % lower if $Y_p\lesssim 0.1$, in the range $\rho\gtrsim 4\times 10^{11}$ g cm^{-3} for the profile Eq. (48). At densities approaching nulear density, the bound state spectrum of nuclei is influenced by the overlap of their wave functions which tends to reduce their abundance below the ones predicted by NSE. This effect cannot be accounted for in a two-nucleon interaction model which therefore ceases to be applicable at such densities.

For the proton-neutron interaction potential $V_S^{np}(r)$ for total spin S we chose the following Gaussian potentials [such that $U_\sigma^{np}=V_1^{np}-V_0^{np}$ and $U^{np}=(V_1^{np}+V_2^{np})/2$ in the notation of Eq. (12)]:

$$V_0^{np}(r)=-33.6e^{-(r/1.77\ \mathrm{fm})^2}\ \mathrm{MeV},$$
$$V_1^{np}(r)=-84.7\,e^{-(r/1.36\ \mathrm{fm})^2}\ \mathrm{MeV}. \quad (49)$$

Its strengths and ranges were fit to reproduce the experimental values for the scattering lengths a_S and effective ranges $r_{\mathrm{eff},S}$ which determine the low-energy expansion of the phase shifts $\delta_{0,S}$ [17]:

$$\cot\delta_{0,S}(s=4p^2)=-\frac{1}{pa_S}+\frac{p}{2}\,r_{\mathrm{eff},S}. \quad (50)$$

As a result, the s-wave proton-neutron scattering cross section predicted by Eq. (49) agrees with the experimental one to within less than 5% in the laboratory energy range between 0 and $\simeq 20$ MeV (see Fig. 1). In addition, the energy of the bound state resulting for $S=1$ coincides with the deuteron binding energy within 5%. A central potential describes the deuteron rather well since the contribution of the D state to the bound state wave function is only about 6%. Finally, we have compared the numbers for the weak neutral-current deuteron break-up cross section resulting from Eq. (31) with calculations in the literature [27]. In the

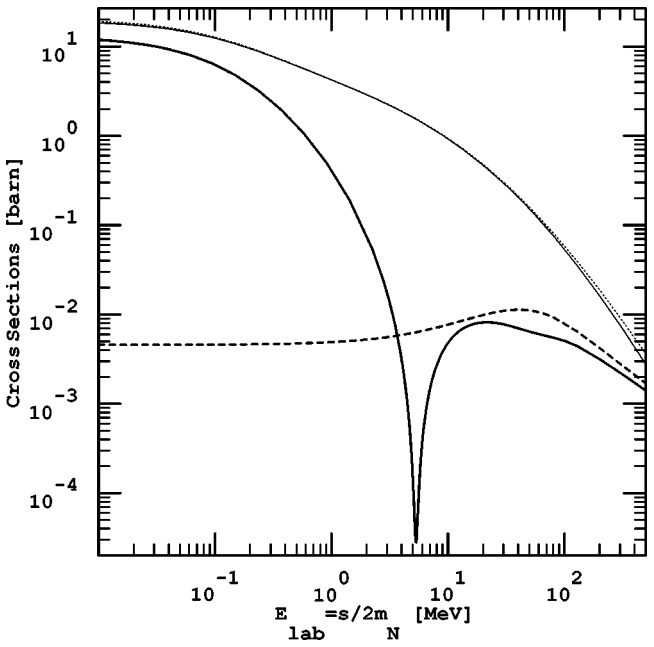

FIG. 1. The s-wave proton-neutron scattering cross section predicted by the potential Eq. (49) (thin solid line) and measured (thin dotted line) as a function of the laboratory kinetic energy $E_{\rm lab}=s/2m_N$. Also shown for this potential is the spin-flip cross section in Born approximation [Eq. (40), thick dashed line] and from phase shift analysis [Eq. (37), thick solid line]. The inverted resonance in the latter curve at $E_{\rm lab}/2\simeq 2.2$ MeV stems from the deuteron bound state.

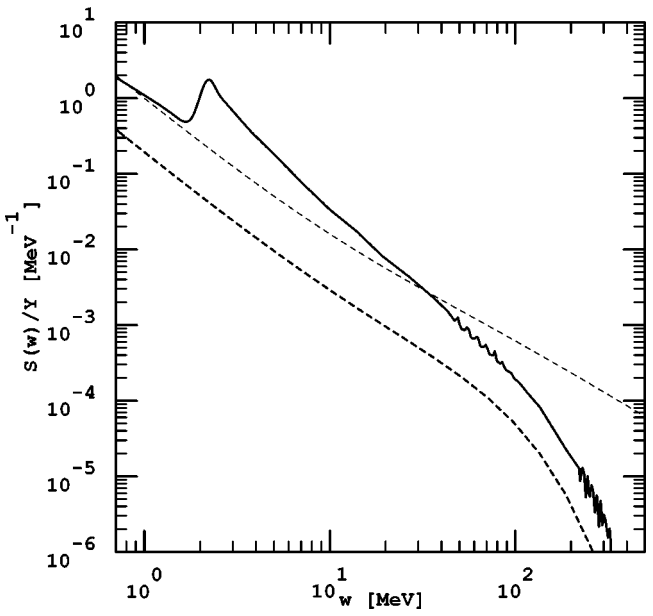

FIG. 2. The contribution from proton-neutron scattering to the dynamical nucleon spin-density structure function $S_\sigma(\omega)/Y$ as a function of ω in the long wavelength limit $k\to 0$ for $\rho=3\times 10^{12}$ g cm^{-3}, $T=7.2$ MeV. Shown are the Born approximation [Eq. (39), thick dashed line] and the result from phase shift analysis [Eq. (28), thick solid line] for the proton-neutron interaction potential Eq. (49) and the estimate Eq. (25) with Eqs. (43)–(46) for an OPE potential in Born approximation (thin dashed line). The resonance at $\omega\simeq 2.2$ MeV from the deuteron binding energy is clearly visible in the thick solid line. The small wiggles on this curve are caused by the finite numerical resolution of the energy eigenvalues of the scattering states. Multiple scattering effects that regularize the ω^{-2} behavior at low ω would here become important for $\omega<\Gamma_\sigma\simeq 1$ MeV, see Fig. 6.

energy range between $\simeq 5$ and 40 MeV we found agreement to within about 10%. This serves as a further check for the correct normalization of our calculation.

Also shown in Fig. 1 is the spin-flip cross section as calculated from the potential Eq. (49) both in Born approximation [Eq. (40)] and numerically from the phase shifts [Eq. (37)]. It is clearly seen that the Born approximation underestimates $\sigma_{\rm sf}$ by far for energies below a few MeV. In contrast, as expected, Born approximation and phase shift analysis for the spin-flip cross section converge at high energies where the second condition in Eq. (1) is asymptotically satisfied.

To compute the nucleon spin-density structure function in phase shift analysis, we calculated radial eigenfunctions up to some maximal orbital angular momentum $l_{\rm max}=3$ above which they are close enough to the free eigenfunctions to make a negligible contribution to Eq. (28). To achieve a sufficient resolution in the energy range of interest, about 500 eigenfunctions had to be computed. We verified that the resulting $S_\sigma(\omega)$ satisfies the f-sum rule Eq. (15) to within 10%. An example for $\rho=3\times 10^{12}$ g cm^{-3}, and $T=7.2$ MeV, values typical for the neutrinosphere, is shown in Fig. 2, along with the Born approximation Eq. (39) for the same potential. Clearly, the Born approximation strongly underestimates S_σ at neutrinosphere temperatures, corresponding to the underestimation of the spin-flip cross section at low energies exhibited in Fig. 1. We have verified that in the limit of weak interaction potentials satisfying the first condition in Eq. (1), the Born approximation agrees well with the phase shift analysis over the whole energy range as expected.

For comparison, Fig. 2 also shows Eq. (25) with the perturbative expressions Eqs. (43)–(46) for the proton-neutron scattering contribution to S_σ based on the OPE potential (thin dashed curve). After all, this curve reproduces the general normalization of the spin-density structure function quite well, but it cannot reproduce the quite prominent deuteron resonance. The nonvanishing pion mass is taken into account in this curve and suppresses it by roughly a factor 2 compared to calculations neglecting the pion mass. Note the steepening at high ω of the curves for the potential Eq. (49) in contrast to $S^{\rm Born}_{\sigma,{\rm OPE}}(\omega)$ which guarantees or violates f-sum integrability, respectively.

The phase space averaged quantities relevant for neutrino interactions and discussed in Sec. II are shown in Figs. 3–5 for the temperature profile Eq. (48) in the density range between 10^{11} g cm^{-3} and 10^{14} g cm^{-3}. Near the lower boundary of this range, the neglect of higher nuclei such as helium is not a good approximation any more. Near the upper boundary, multiple nucleon scattering [10,24] and saturation of nucleon spin fluctuations [16] start to become important as Γ_σ becomes comparable to T [see Eq. (23)], as can be seen from Fig. 6. Furthermore, modifications of nuclear bound states due to overlap of their wave functions, which is an additional many-body effect, becomes important at these densities, as mentioned above.

We stress again that due to the presence of bound states the spin-density structure function calculated by phase shift

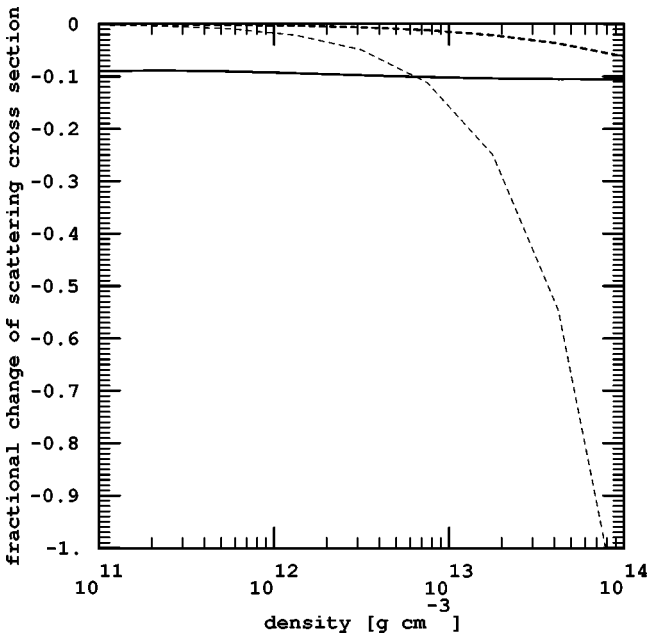

FIG. 3. The contribution from proton-neutron scattering to the fractional change $\delta\langle\sigma_A\rangle/(\sigma_0 Y)$ of the average total axial-vector current neutrino-nucleon scattering cross section [see Eq. (21)]. This is shown as a function of ρ for the profile Eq. (48). The line key is identical to Fig. 2. For the phase shift analysis Eq. (38) was used for N_σ, whereas $N_\sigma=0$ was used for the Born approximations.

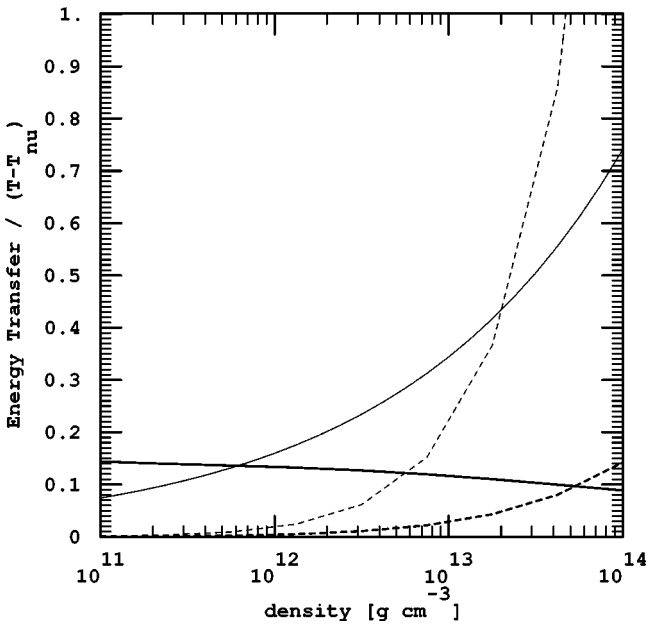

FIG. 4. The contribution from proton-neutron scattering to the average energy transfer in axial-vector neutrino-nucleon scattering, normalized to the difference of neutrino and medium temperatures, $\langle\Delta\varepsilon\rangle/Y(T_\nu-T)$ [see Eq. (18)]. This is shown as a function of ρ for the profile Eq. (48). The line key is identical to Fig. 2. In addition, the thin solid line shows the Y independent contribution from recoil, Eq. (19). The normalization relative to the inelastic contributions that are proportional to Y corresponds to $Y=1$.

analysis and weak interaction rates computed from it do not exhibit a simple scaling behavior with density and/or temperature, as discussed below Eq. (29).

We note from Eqs. (21), (38), and (47) that the scattering cross section reduction shown in Fig. 3 is proportional to Y. The main contribution to N_σ comes from the $S=1$ deuteron bound state

$$N_{\sigma,d}=\frac{C_{A,p}C_{A,n}}{(C_{A,p}-C_{A,n})^2}(1-f_u)\frac{Y}{3}\simeq -0.083(1-f_u)Y \tag{51}$$

and is roughly half the size of the second term in Eq. (21). The negative contribution to $\langle\sigma_A\rangle$ results from the opposite sign of $C_{A,p}$ and $C_{A,n}$ and corresponds to the fact that the cross section for elastic scattering on deuterons is significantly smaller than that on free nucleons. The resulting predicted total cross section reduction is almost constant $\simeq 10\%$ over the whole density range shown in Fig. 3. Furthermore, we note that Eqs. (18) and (19) imply that $\langle\Delta\varepsilon\rangle\propto T_\nu-T$ for $|T_\nu-T|\ll T$ which makes it convenient to plot the ratio of these quantities in Fig. 4.

Clearly, near the low end of the temperature and density range considered, the Born approximations for both the potential Eq. (49) and OPE tend to predict substantially lower absolute values for all of the quantities shown in Figs. 3–6. For the potential Eq. (49) this is related to the fact that the spin-flip cross section $\sigma_{\rm sf}(s)$ is strongly underestimated by the Born approximation below a few MeV (see Fig. 1). In turn, this leads to an underestimation of the spin-flip rate Eq. (36) for temperatures below a few MeV, and the spin fluctuation rate that satisfies $\Gamma_\sigma/\Gamma_{\rm sf}\simeq\Gamma_\sigma^{\rm Born}/\Gamma_{\rm sf}^{\rm Born}$ $=27/10(C_p-C_n)^2/C^2$ [see Eq. (41)] and characterizes $S_\sigma(\omega)$ via Eq. (25). At higher temperatures and densities the predictions based on phase shift analysis and Born approximation for the potential Eq. (49) are closer because the effective potential ''seen'' by the scattering nuclei becomes smaller relative to their kinetic energy and the second condition for applicability of perturbation theory in Eq. (1) be-

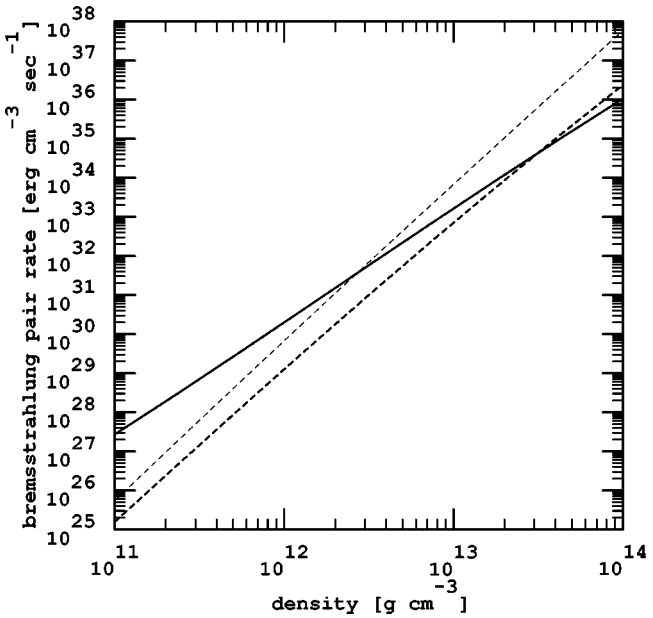

FIG. 5. The contribution from proton-neutron scattering to the neutrino pair emissivity $Q_{\nu\bar{\nu}}/Y$ [see Eq. (22)], shown as a function of ρ for the profile Eq. (48). The line key is identical to Fig. 2.

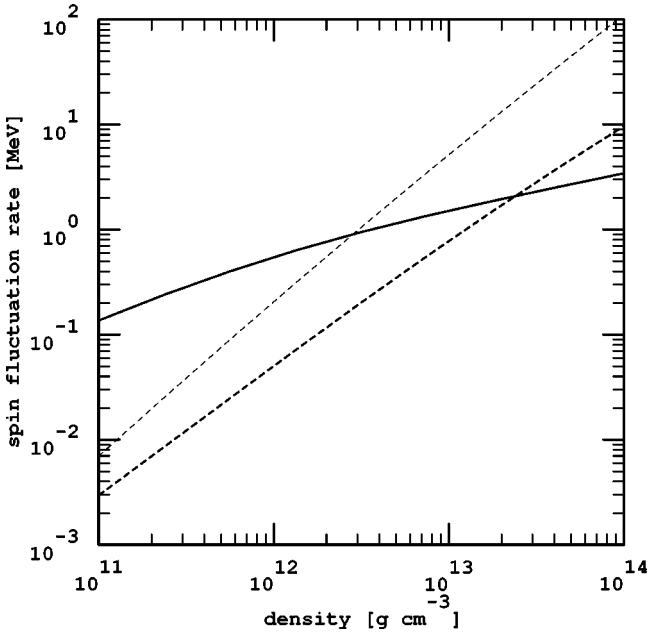

FIG. 6. The spin fluctuation rate Γ_σ/Y as a function of ρ for the profile Eq. (48). The line key is identical to Fig. 2.

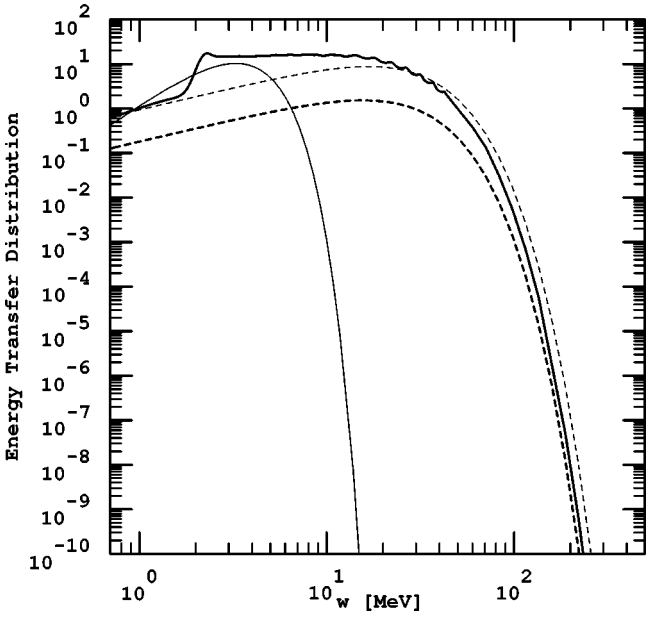

FIG. 7. The contribution from proton-neutron scattering to the distribution of energy transfers ω in axial-vector neutrino-nucleon scattering per logarithmic interval in ω and difference in neutrino and medium temperature in arbitrary units, for $\rho=3\times10^{12}$ g cm^{-3}, and $T=7.2$ MeV. According to Eq. (18), this is proportional to $[S_\sigma(xT)/Y]x^3(1+x/2+x^2/12)e^{-x}$, where $S_\sigma(\omega)$ was shown in Fig. 2 for the same conditions with identical line key. In addition, the thin solid line was obtained from the Y independent recoil structure function, Eq. (32), for a typical thermal momentum transfer $k=3T$. The normalization relative to the inelastic contributions that are proportional to Y corresponds to $Y=1$.

comes asymptotically satisfied. They do not converge, however, because the deuteron abundance increases within our two-nucleon interaction approximation which eventually becomes inapplicable.

Close to the neutrinosphere, at densities of a few 10^{12} g cm^{-3}, predictions by our phase shift analysis for the potential Eq. (49) and by the Born approximation for the OPE potential for the integrated quantities shown in Figs. 3–6 agree reasonably well. In particular, our results predict that for $\rho\lesssim10^{12}$ g cm^{-3} the average inelastic neutrino-nucleon energy transfer $\langle\Delta\varepsilon\rangle$ is comparable to the recoil energy $\langle\Delta\varepsilon\rangle_{\rm recoil}$ (see Fig. 4), as first suggested in Refs. [10,9] for conditions near the neutrinosphere. These energy transfers are, however, differently distributed with a much longer tail to large-energy transfers, as shown in Fig. 7, and their average value has a much weaker temperature and density dependence than predicted by the calculations for OPE in Born approximation.

We have furthermore checked that the results for S_σ calculated from the phase shift analysis Eq. (28) are insensitive to the detailed shape of $U_\sigma^{np}(r)$ as long as it reproduces the experimental phase shifts in the corresponding energy range. In particular, properties of the potential at short distances r influence $S_\sigma(\omega)$ only for $\omega=p^2/m_N\gtrsim1/(m_Nr^2)$. For the conditions near the neutrinosphere it is therefore sufficient that the potential reproduces nucleon-nucleon scattering up to a few tens of MeV.

By comparing with the experimentally measured rates for the process $p+p\to p+p+\pi_0$, it was argued in Ref. [28] that the OPE potential in Born approximation should describe the axion emission process $p+p\to p+p+a$ rather well even in the supernova core. This should hold true for other related weak interaction rates as well. This argument, however, cannot be extended to the analogous processes Eqs. (2) and (3) involving neutrons and protons that have been the subject of the present paper: Whereas only the tensor contribution of the two-nucleon interaction potential is relevant for processes involving only one nucleon species, the reaction involving a proton and a neutron also depends on the central part of the potential and is therefore not related to the former by simple isospin symmetry. Indeed, the fact mentioned in Sec. IV that the OPE potential leads to an unphysical short distance behavior for proton-neutron interactions, but not for interactions among identical flavors, is related to this. One can therefore not expect proton-neutron bremsstrahlung calculations adopting the OPE potential in Born approximation to yield reliable estimates of weak interaction rates at high temperatures and densities.

Indeed, towards the center of the hot neutron star, at densities approaching nuclear density and $T\gtrsim20$ MeV, predictions for the quantities shown in Figs. 3–5 by the OPE potential in Born approximation are at least 10 times higher than corresponding predictions based on the potential Eq. (49) for which Born approximation and phase shift analysis become rather similar. This demonstrates that in this environment weak interaction rates indeed become quite sensitive to the short-distance behavior of the two-nucleon interaction potential which is different for these two potentials. This can have important ramifications for neutrino opacities and axion and neutrino pair emissivities in the supernova core that are usually based on these OPE calculations [11,12]. Whereas calculations assuming an OPE potential should be a reasonable approximation in the context of a ''cold'' neutron star this is not necessarily the case for the much higher thermal energies involved in a hot protoneutron star. Neutrino opacities govern the cooling time scale of the

protoneutron star [25] while axion emissivities determine axion mass bounds based on supernovae [26]. Apart from taking into account many-body effects such as multiple scattering [24,10,16], a more reliable calculation of these quantities thus requires to use nuclear potentials that fit nucleon-nucleon scattering data also at energies above a few tens of MeV to ensure the correct small distance behavior. We leave that to a separate study.

Finally, to qualitatively compensate for the overestimation of the deuterium abundance by our model at high densities, we checked how our results change when any contributions from bound states are neglected. The curves shown in Figs. 3–6 for the potential Eq. (49) then have a more similar shape, with the magnitudes predicted by the phase shift analysis being larger than the ones based on the Born approximation by a factor that varies monotonously between $\simeq 10$ near the low end, and $\simeq 2$ near the high end of the density range considered.

VI. SUMMARY AND CONCLUSIONS

We have discussed weak axial-vector neutral-current interactions involving nucleons in hot nondegenerate nuclear matter at temperatures between a few MeV and about 25 MeV, and densities between $\simeq 10^{11}$ and $\simeq 10^{14}$ g cm^{-3}, i.e., for conditions given in the vicinity of the neutrinosphere in a type-II supernova. To describe such interactions in the limit of nonrelativistic nucleons we adopted the structure function formalism for the nucleon spin-density. We studied the reduction of the average total axial-vector current neutrino-nucleon scattering cross section, the associated average energy transfer, and the neutrino pair emissivity, all of which are governed by the nucleon spin fluctuations caused by the spin-dependent nucleon-nucleon interactions. To lowest order in the nucleon-nucleon interactions, i.e., in Born approximation, this is represented by nucleon bremsstrahlung. We have shown, however, that near the low end of the temperature and density range considered here, the Born approximation is in general a reliable estimate neither for these quantities nor for the spectral shape of the spin-density structure function which determines the distribution of the energy exchanged with the nuclear matter in scattering and pair processes. As an alternative, we have performed computations using exact two-nucleon wave functions for a spherically symmetric two-nucleon interaction potential that was fit to experimental data. In this case, only proton-neutron interactions contribute to inelastic weak neutral-current interactions with nucleons. We also compared our calculations with results for the corresponding contribution based on the usually adopted OPE potential in the Born approximation. In general, near the low end of the temperature and density range considered, the OPE calculations tend to underestimate the quantities discussed here, whereas near the high end an overestimation is indicated. We confirm that for the conditions near the neutrinosphere the average energy transfer in axial-vector neutrino-nucleon scattering can be comparable to the recoil energy, as suggested by the OPE calculations.

The formalism presented here can be extended to two-nucleon potentials that are not spherically symmetric as well as to finite momentum transfer [see Eq. (27)].

Our results might have a significant impact on the formation of neutrino spectra from type-II supernovae. A quantitative understanding will, however, require detailed numerical simulations. Qualitatively, the ''energy'' sphere is located where the rates of processes that change neutrino energies and numbers equal the diffusion rate [29,2]. A rough estimate employing the new rates from our phase shift analysis indicates no significant change in the location of the energy spheres of ν_e, $\overline{\nu_e}$, and muon and τ neutrinos at $T\simeq 4$, $T\simeq 4.6$, and $T\simeq 7.5$ MeV, respectively. However, the additional energy transfer in inelastic neutrino-nucleon scattering and the weaker fall off of bremsstrahlung pair rates at low temperatures and densities (see Figs. 4 and 5) suggests an increased efficiency of energy exchange with the medium between the energy spheres and the surface of last scattering at $T\simeq 4$ MeV, and thus a softening of the spectra. Since this applies equally to all neutrino flavors, this could also result in more similar spectral temperatures for the different flavors and could be tested by the next generation neutrino observatories once a supernova is detected.

Finally, we demonstrated that weak interaction rates in the hot supernova core are sensitive to the small distance behavior of the nucleon-nucleon interaction potential which, at least for proton-neutron interactions, is not well described by the usually adopted OPE potential. This, apart from many-body effects, should be taken into account in future investigations.

ACKNOWLEDGMENTS

I am grateful to Georg Raffelt and Hans-Thomas Janka for many discussions on this subject and for useful comments on the manuscript. This work was supported, in part, by the Deutsche Forschungsgemeinschaft under Grant No. SFB 375, by the U.S. DOE, NSF, and NASA at the University of Chicago, and by the U.S. DOE and by NASA through Grant No. NAG 5-2788 at Fermilab.

[1] For a review see, e.g., D. N. Schramm and J. W. Truran, Phys. Rep. **189**, 89 (1990).

[2] H.-Th. Janka, Astropart. Phys. **3**, 377 (1995).

[3] See, e.g., R. W. Mayle, J. R. Wilson, and D. N. Schramm, Astrophys. J. **318**, 288 (1987); H.-Th. Janka and W. Hillebrandt, Astron. Astrophys. Suppl. Ser. **78**, 375 (1989); E. S. Myra and A. Burrows, Astrophys. J. **364**, 222 (1990).

[4] N. Iwamoto and C. J. Pethick, Phys. Rev. D **25**, 313 (1982).

[5] E. G. Flowers, P. G. Sutherland, and J. R. Bond, Phys. Rev. D **12**, 315 (1975); P. Haensel and A. J. Jerzak, Astron. Astrophys. **179**, 127 (1987); K. Lim and C. J. Horowitz, Nucl. Phys. **A501**, 729 (1989); C. J. Horowitz and K. Wehrberger, *ibid.* **A531**, 665 (1991); Phys. Rev. Lett. **66**, 272 (1991).

[6] R. F. Sawyer, Phys. Rev. D **11**, 2740 (1975); Phys. Rev. C **40**, 865 (1989).

[7] C. J. Horowitz and K. Wehrberger, Phys. Lett. B **266**, 236

(1991); G. Röpke, K. Morawetz, and T. Alm, *ibid.* **313**, 1 (1993).
[8] R. F. Sawyer, Phys. Rev. Lett. **75**, 2260 (1995).
[9] G. G. Raffelt, D. Seckel, and G. Sigl, Phys. Rev. D **54**, 2784 (1996).
[10] H.-Th. Janka, W. Keil, G. Raffelt, and D. Seckel, Phys. Rev. Lett. **76**, 2621 (1996).
[11] B. L. Friman and O. V. Maxwell, Astrophys. J. **232**, 541 (1979).
[12] R. P. Brinkmann and M. S. Turner, Phys. Rev. D **38**, 2338 (1988).
[13] G. G. Raffelt and D. Seckel, Phys. Rev. D **52**, 1780 (1995).
[14] See, e.g., L. I. Schiff, *Quantum Mechanics*, 2nd ed. (McGraw-Hill, New York, 1955), pp. 169–170.
[15] For a review on axions see, e.g., G. G. Raffelt, Phys. Rep. **198**, 1 (1990).
[16] G. Sigl, Phys. Rev. Lett. **76**, 2625 (1996).
[17] See, e.g., P. Marmier and E. Sheldon, *Physics of Nuclei and Particles* (Academic, New York, 1970).
[18] See, e.g., D. Forster, *Hydrodynamic Fluctuations, Broken Symmetry, and Correlation Functions* (Benjamin, New York, 1975).
[19] G. G. Raffelt and T. Strobel, Phys. Rev. D **55**, 523 (1997).
[20] D. L. Tubbs, Astrophys. J. **231**, 846 (1979).
[21] G. G. Raffelt, *Stars as Laboratories for Fundamental Physics* (University of Chicago Press, Chicago, 1996).
[22] L. D. Landau and I. Ja. Pomeranchuk, Dokl. Akad. Nauk SSSR **92**, 535 (1953); **92**, 735 (1953); E. L. Feinberg and I. Ja. Pomeranchuk, Nuovo Cimento Suppl. **3**, 652 (1956).
[23] J. Knoll and D. M. Voskresensky, Phys. Lett. B **351**, 43 (1995).
[24] G. G. Raffelt and D. Seckel, Phys. Rev. Lett. **67**, 2605 (1991).
[25] W. Keil, H.-Th. Janka, and G. G. Raffelt, Phys. Rev. D **51**, 6635 (1995).
[26] W. Keil, H.-Th. Janka, D. N. Schramm, G. Sigl, M. S. Turner, and J. Ellis, Phys. Rev. D **56**, 2419 (1997).
[27] J. N. Bahcall, K. Kubodera, and S. Nozawa, Phys. Rev. D **38**, 1030 (1988).
[28] M. S. Turner, H. Kang, and G. Steigman, Phys. Rev. D **40**, 299 (1989).
[29] G. Sigl and M. S. Turner, Phys. Rev. D **51**, 1499 (1995).